

^{68}Ga -Labeled Benzothiazole Derivatives for Imaging $\text{A}\beta$ Plaques in Cerebral Amyloid Angiopathy

Truc T. Huynh, Yujue Wang, Karna Terpstra, Hong-Jun Cho, Liviu M. Mirica,* and Buck E. Rogers*

Cite This: *ACS Omega* 2022, 7, 20339–20346

Read Online

ACCESS |



Metrics & More

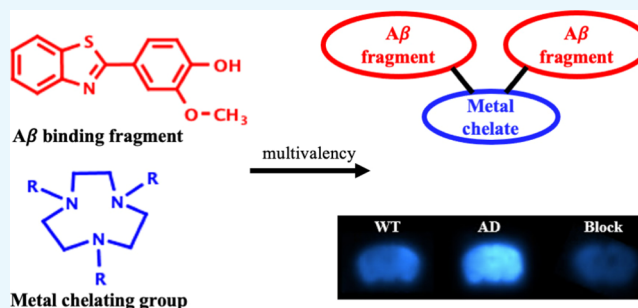


Article Recommendations



Supporting Information

ABSTRACT: Timely diagnostic imaging plays a crucial role in managing cerebral amyloid angiopathy (CAA)—the condition in which amyloid β is deposited on blood vessels. To selectively map these amyloid plaques, we have designed amyloid-targeting ligands that can effectively complex with $^{68}\text{Ga}^{3+}$ while maintaining good affinity for amyloid β . In this study, we introduced novel 1,4,7-triazacyclononane-based bifunctional chelators (BFCs) that incorporate a benzothiazole moiety as the $\text{A}\beta$ -binding fragment and form charged and neutral species with $^{68}\text{Ga}^{3+}$. In vitro autoradiography using 5xFAD and WT mouse brain sections (11-month-old) suggested strong and specific binding of the ^{68}Ga complexes to amyloid β . Biodistribution studies in CD-1 mice revealed a low brain uptake of 0.10–0.33% ID/g, thus suggesting CAA.



^{68}Ga -labeled novel BFCs as promising candidates for detecting

INTRODUCTION

Cerebral amyloid angiopathy (CAA) is the condition in which amyloid β is built on the walls of the arteries in the brain, thus allowing blood to leak out and causing hemorrhagic strokes in the elderly.^{1,2} This differs from Alzheimer's disease (AD) in which amyloid β is deposited in the brain parenchyma and requires targeted agents to cross the blood–brain barrier (BBB).³ CAA is present in a majority of people with AD (78–98%), and both are associated with the amyloid disposition and eventual neurological decline.^{4–6} Unfortunately, there are currently no effective prevention or treatment strategies for CAA. To date, a definitive diagnosis of CAA can only be made through a post-mortem examination of the brain; therefore, probes for the imaging of amyloid β are highly desirable. This led to the development of a variety of chemical scaffolds as $\text{A}\beta$ -imaging tracers such as the thioflavin T analogues, chalcone, and curcumin derivatives that displayed high binding affinity toward $\text{A}\beta$ aggregates.^{7–10}

Multiple researchers have explored the development of positron emission tomography (PET) radiopharmaceuticals that target amyloid plaques. Pittsburgh compound B [^{11}C]C-PiB ($T_{1/2} = 20$ min, $\beta^+ \approx 100\%$, $E_{\text{max}} = 0.96$ MeV) is widely studied as the first agent to show increased retention in regions containing high levels of amyloid plaques.^{11,12} Several ^{18}F -labeled PET tracers ($T_{1/2} = 110$ min, $\beta^+ = 97\%$, $E_{\text{max}} = 0.63$ MeV) have also been investigated and have more potential for broader clinical applications due to their longer half-life. In fact, three ^{18}F ligands have been approved for clinical use of imaging amyloid plaque density in patients by regulatory authorities in both Europe and the United States, including

[^{18}F]F-AV-45 (Florbetapir), [^{18}F]F-BAY94–9172 (Florbetaben), and [^{18}F]3'-F-PiB (Flutemetamol).^{13–15} However, radiolabeling schemes of ^{11}C and ^{18}F complexes often require complex multistep synthesis and readily cross the BBB, which means they cannot distinguish between AD and CAA. The BBB serves to separate the brain's blood vessels and components that make up brain tissues. Previous studies proposed that the selectivity of radiolabeled compounds for CAA stems from limited BBB penetration, thus restricting access to brain parenchyma where amyloid β is deposited for AD.^{16,17} Therefore, the design of novel radiopharmaceuticals that have more straightforward radiolabeling schemes such as the metal-based radionuclide ^{68}Ga and have low BBB permeability would be desirable.

Compared to ^{11}C and ^{18}F , ^{68}Ga ($T_{1/2} = 68$ min, $\beta^+ = 89\%$, $E_{\text{max}} = 1.92$ MeV) is a generator produced positron-emitting radionuclide, thus allowing for the distribution of PET imaging agents independent of on-site cyclotrons. The comparatively long half-life of the parent radionuclide (^{68}Ge) of 271 days can provide ^{68}Ga for an extended period of 6 months and multiple elutions can be performed in a day, resulting in ^{68}Ga being a more cost-effective and reliable source of radionuclides.¹⁸

Received: April 15, 2022

Accepted: May 20, 2022

Published: June 6, 2022



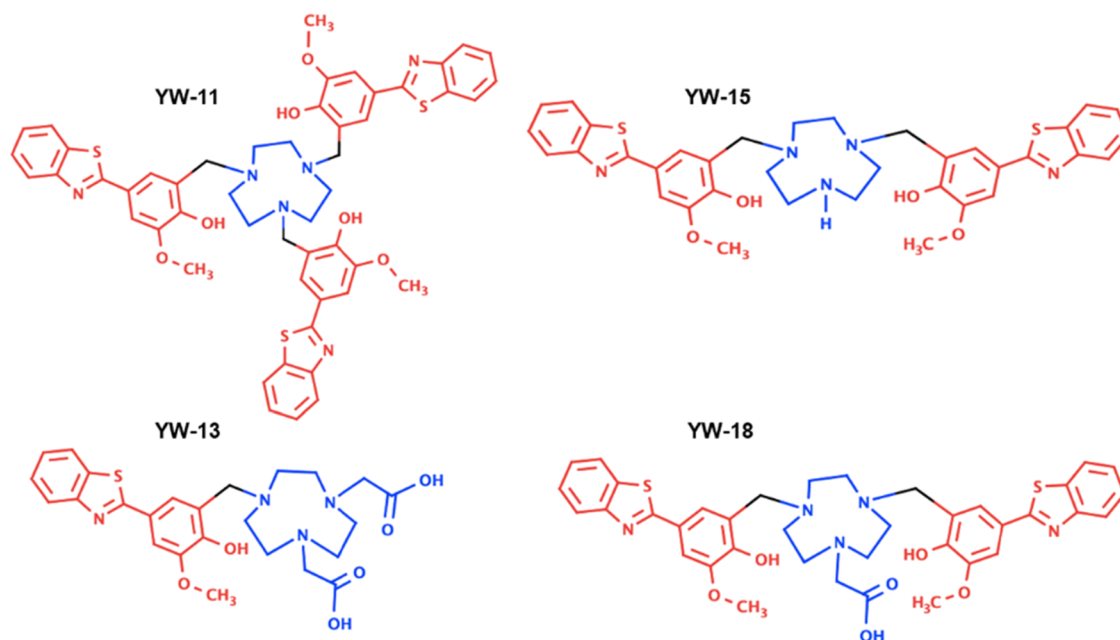
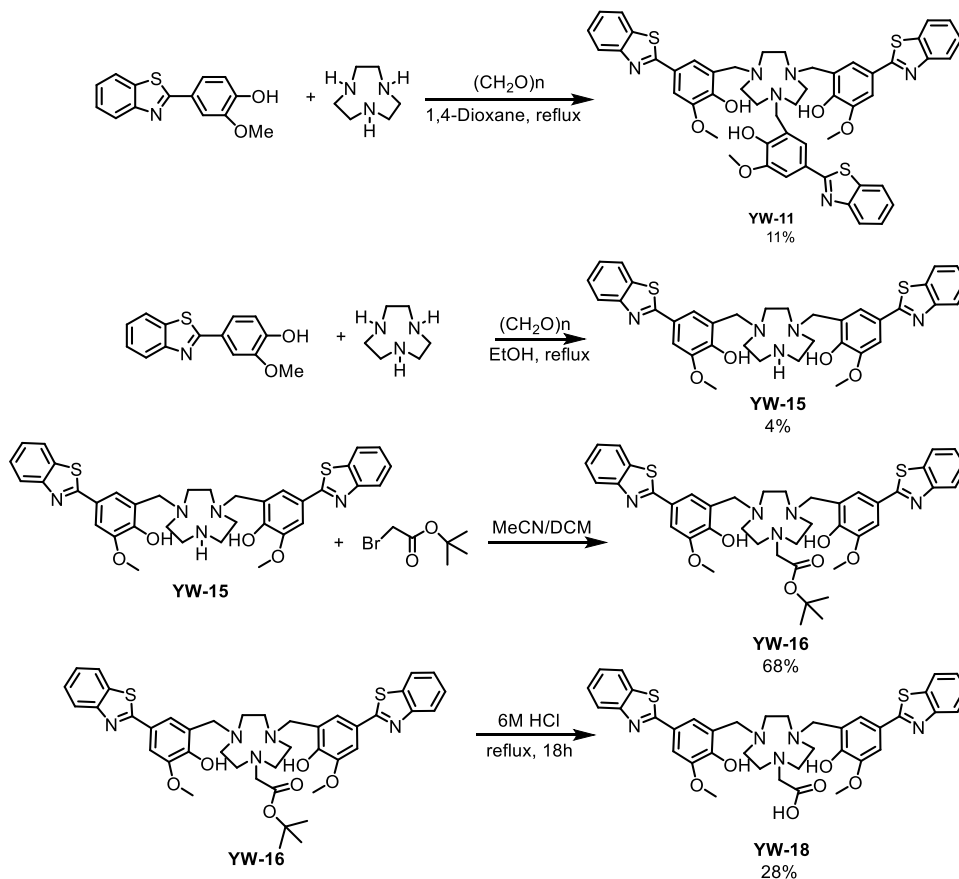


Figure 1. Novel TACN-based BFCs examined in this study. The amyloid-interacting and metal-binding fragments are shown in red and blue, respectively.

Scheme 1. Synthesis Routes for the Ligands Investigated



Additionally, ^{68}Ga has well-established coordination chemistry and fast and selective complex formation for direct labeling of biomolecules, thus making it an attractive option for amyloid β ($A\beta$) imaging.¹⁹

Multiple gallium-based imaging agents have been proposed and tested in vitro and in vivo for the imaging of $A\beta$ plaques. Zha et al. described a series of ^{68}Ga -labeled styrylpyridine derivatives with N,N' -bis[2-hydroxy-5-(carboxyethyl)benzyl]-ethylenediamine- N,N' -diacetic acid (HBED-CC) as the metal-

chelating agent, which exhibited excellent affinity toward amyloid β on post-mortem brain sections from patients diagnosed with AD.¹⁷ Watanabe et al. reported ⁶⁸Ga-labeled benzofuran derivatives conjugated with metal-chelating 1,4,7,10-tetraazacyclododecane-1,4,7,10-tetraacetic acid (DOTA), and fluorescence staining of Tg2576 mouse brain sections incubated in non-radioactive gallium complexes revealed clear staining of amyloid β plaques.²⁰ Cressier et al. also introduced ⁶⁸Ga-labeled PiB derivatives for the imaging of amyloid β plaques; however, in vitro autoradiography in human brain sections revealed their weak affinity for amyloid deposits.²¹ On the other hand, different organic motifs such as curcumin and chalcone radiolabeled with gallium were evaluated as $A\beta$ -binding diagnostic agents.^{22–25} For example, Asti et al. reported ⁶⁸Ga-labeled curcuminoids that showed good affinity to synthetic β -amyloid fibrils.²² Chauhan et al. explored ⁶⁸Ga-labeled chalcone-based probes, in which an in vitro binding assay displayed excellent binding affinity to $A\beta_{42}$ aggregates.²⁴ These compounds could be useful for imaging CAA, but most have not been evaluated further. [⁶⁸Ga]Ga-p14-032 that utilized HBED-CC as a chelator was evaluated in patients with probable CAA compared with healthy patients and those with AD, and PET scans revealed preferable binding of this radiolabeled complex toward CAA.²⁶

Here, we investigated a series of gallium-coordination bifunctional chelators (BFCs) with an $A\beta$ -binding 2-(4-hydroxyphenyl)-benzothiazole moiety and metal-chelating 1,4,7-triazacyclononane (TACN) ligands (Figure 1). The TACN backbone was reported to efficiently chelate various metal ions including Cu^{2+} , Ga^{3+} , Sc^{3+} , and In^{3+} . A comparative study showed that TACN derivatives compete favorably for Ga^{3+} in reactions with HBED and DOTA.²⁷ ⁶⁸Ga-labeled biomolecules with NOTA (a TACN derivative) are also superior in vivo in comparison to HBED and DOTA.^{28,29} In this study, multiple $A\beta$ -binding moieties were generated on the N-atoms of TACN metal-binding fragments to increase the affinity of radiolabeled complexes to amyloid β .^{30–36} Multi-valent binding has been reported to enhance binding affinity. Iikuni et al. have evaluated bivalent [^{99m}Tc]-Tc-Ham complexes and confirmed that bivalency led to superior binding affinity for amyloid β when compared to monovalent complexes.¹⁶ Cho et al. have recently proposed a series of divalent BFCs that showed enhanced binding affinity toward $A\beta$ aggregates when comparing the autoradiographic images of 5xFAD mouse brain sections incubated with the mono- or divalent ⁶⁴Cu complexes.³⁴ This study evaluated novel TACN-based BFCs for CAA imaging by examining the radiochemistry with ⁶⁸Ga, affinity toward amyloid β in 5xFAD mice brain sections, and biodistribution in normal CD-1 mice.

RESULTS

Design and Syntheses of BFCs. YW-13 was synthesized as previously described.³⁵ The synthesis of the other compounds is outlined in Scheme 1. To further improve the binding affinity for amyloid β , multiple $A\beta$ -binding fragments were conjugated to the TACN backbone, thus generating the bivalent YW-15 and trivalent YW-11 product, respectively. An additional carboxylate arm was present in the bivalent YW-18, which served to enhance the metal-chelating ability of this BFC. Characterization of these compounds was performed through ESI-MS and NMR (Figures S1–S12).

Histological Staining of 5xFAD Mouse Brain Sections. Figure 2 depicts the staining of 5xFAD brain sections with

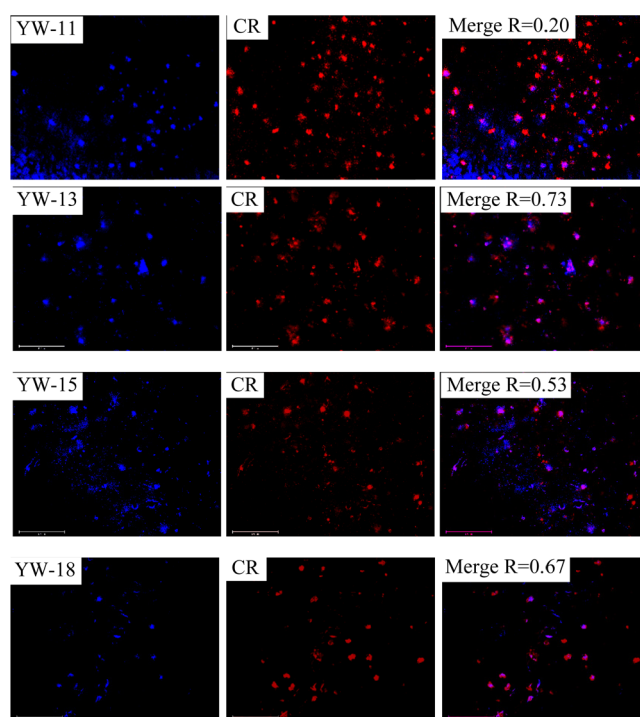


Figure 2. A panel of images from fluorescence microscopy that show stained 5xFAD brain sections previously incubated with YW-11, YW-13, YW-15, and YW-18 (left), Congo Red (middle), and merged images (right). Scale bar: 125 μm . Magnification: 20 \times .

novel BFCs and sequentially Congo Red. Intense fluorescence signals were detected upon the incubation of 11-month-old 5xFAD mouse brain sections with BFC solution (left) and with Congo Red (middle). YW-13, YW-15, and YW-18 show fairly good colocalization of the two panels, as indicated by Pearson's correlation coefficients of 0.53–0.73, suggesting that these BFCs exhibit good affinity for the amyloid aggregates.^{30–36} In contrast, YW-11 exhibits weak colocalization with the Congo Red-stained region (Pearson's correlation coefficient = 0.2).

The specific $A\beta$ binding of BFCs is further confirmed upon the incubation of 5xFAD mouse brain sections (11-month-old) with the AF594-HJ3.4 antibody (Figure 3). Fluorescence images show that the colocalization between YW-13 and YW-18 (left) and the HJ3.4 antibody (middle) is highly consistent with the Congo Red staining study. There is a slight improvement in the colocalization between YW-15 and the HJ3.4 antibody with Pearson's correlation coefficients of 0.69 as compared to 0.53 for Congo Red staining.

Radiolabeling of BFCs. BFCs were radiolabeled with ⁶⁸Ga at 95 $^{\circ}\text{C}$ for 15 min in NH_4OAc buffer pH 5.5, resulting in products of high radiochemical yield and radiochemical purity (>95%), as illustrated by radio-high-pressure liquid chromatography (HPLC) except for YW-11 which is 90% pure (Figure S13). A single radiolabeled peak was observed for YW-13, YW-15, and YW-18 when complexed with ⁶⁸Ga. In the case of YW-11, the complexed product contained two distinct radiolabeled peaks with the minor peak likely due to the loss of one pendant arm during the radiolabeling process.

Lipophilicity Studies. The $\log D_{\text{oct}}$ values for radiotracers were determined using octanol–PBS partitioning as shown in Table 1. [⁶⁸Ga]Ga-YW-18 has the highest $\log D_{\text{oct}}$ value of 1.66 ± 0.05 , followed by [⁶⁸Ga]Ga-YW-11 of 1.58 ± 0.09 ,

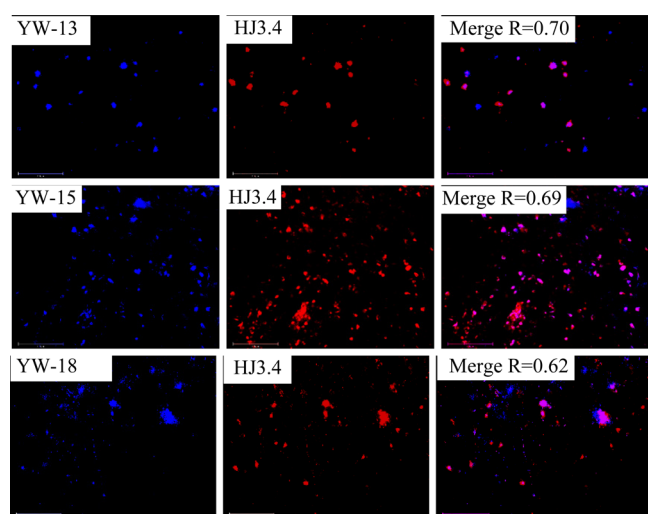


Figure 3. A panel of images from fluorescence microscopy that show stained 5xFAD brain sections previously incubated with YW-13, YW-15, and YW-18 (left), AF594-HJ3.4 (middle), and merged images (right). Scale bar: 125 μm . Magnification: 20 \times .

$[^{68}\text{Ga}]\text{Ga-YW-15}$ of 1.24 ± 0.05 , and $[^{68}\text{Ga}]\text{Ga-YW-13}$ of 0.14 ± 0.02 .

Table 1. Properties of ^{68}Ga -Labeled Ligands Expressed as $\log D_{\text{oct}}$ Values ($n = 10$, Mean \pm SD)

ligand	molecular weight (g/mol)	$\log D_{\text{oct}}$
$[^{68}\text{Ga}]\text{Ga-YW-11}$	1005.1	1.58 ± 0.09
$[^{68}\text{Ga}]\text{Ga-YW-13}$	582.1	0.14 ± 0.02
$[^{68}\text{Ga}]\text{Ga-YW-15}$	735.1	1.24 ± 0.05
$[^{68}\text{Ga}]\text{Ga-YW-18}$	793.1	1.66 ± 0.05

In Vitro Autoradiography Studies. The brain sections of 5xFAD and WT mice (11-month-old) were utilized and stained with radioactive complexes (Figure 4). The autoradiographic images showed effective blocking after 5xFAD brain sections were incubated with excess 2-(4-hydroxyphenyl)-benzothiazole, indicating that ^{68}Ga -radiolabeled complexes were competing for the same amyloid-binding sites. Autoradiographic images revealed more intense signals in 5xFAD brain sections compared to those in WT ones when incubated with ^{68}Ga -radiolabeled complexes, thus confirming the specific binding property of the BFCs to amyloid plaques. Interestingly, even the ^{68}Ga complex of YW-11, which itself does not bind specifically to $A\beta$ plaques, does exhibit specific binding, suggesting that the conformation and charge of the ^{68}Ga complex lead to an improved binding to amyloid plaques. Compared to other BFCs, ^{68}Ga -labeled bivalent complexes exhibited the highest non-specific binding as observed in WT brain sections. Quantitative data showed that $[^{68}\text{Ga}]\text{Ga-YW-11}$ had the highest intensity ratio of 5xFAD to WT brain sections of 4.0, compared to 2.9 for $[^{68}\text{Ga}]\text{Ga-YW-15}$, 3.0 for $[^{68}\text{Ga}]\text{Ga-YW-18}$, and 2.0 for $[^{68}\text{Ga}]\text{Ga-YW-13}$.

Biodistribution Studies. Experiments in vivo using CD-1 mice demonstrated low brain uptake after intravenous injection of ^{68}Ga -radiolabeled complexes (Figure 5). The brain uptake of $[^{68}\text{Ga}]\text{Ga-YW-11}$ was $0.10 \pm 0.03\%$ ID/g at 2 min, reducing to $0.05 \pm 0.02\%$ ID/g at 2 h. The brain uptake of $[^{68}\text{Ga}]\text{Ga-YW-15}$ was $0.26 \pm 0.12\%$ ID/g at 2 min, slowly clearing to $0.07 \pm 0.02\%$ ID/g at 1 h and $0.03 \pm 0.00\%$ ID/g at

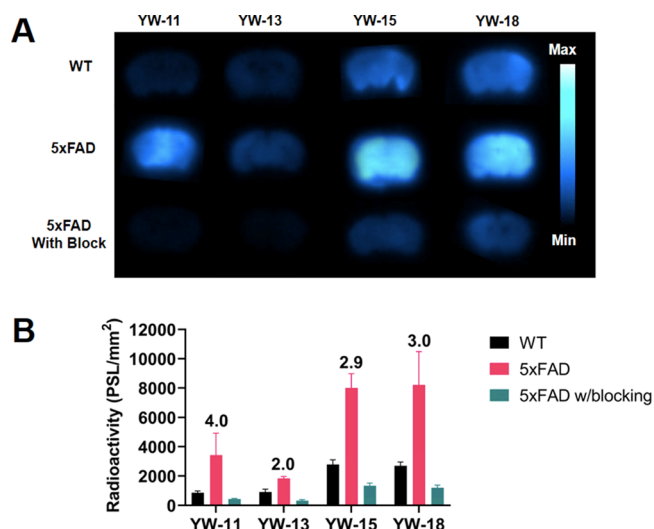


Figure 4. In vitro autoradiography of 5xFAD mice and WT mice ($n = 3$, bars = SD). (A) Autoradiographic images of 11-month-old brain sections incubated in 100 μCi ^{68}Ga -labeled radiotracers for 1 h with or without blocking. (B) Relative optical intensity (PSL/ mm^2) of brain sections derived from autoradiograms. The numbers above the bars are the ratios of red bars to black bars.

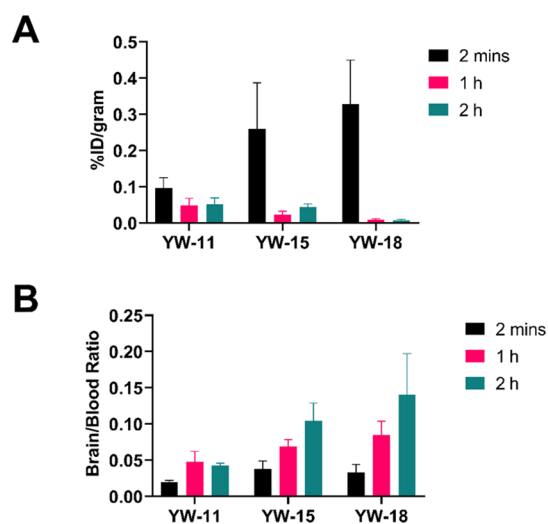


Figure 5. Brain uptake of ^{68}Ga -labeled BFCs in CD-1 mice. (A) Radiotracer uptake in brain after intravenous injection of 10 μCi ^{68}Ga -labeled radiotracers ($n = 3$, %ID/g; bars = SD) and (B) brain-to-blood ratios derived from biodistribution profile.

2 h. Compared to the other two, $[^{68}\text{Ga}]\text{Ga-YW-18}$ possessed the highest brain uptake at 2 min ($0.33 \pm 0.12\%$ ID/g), which rapidly washed out to $0.01 \pm 0.00\%$ ID/g at 2 h. With regard to the brain-to-blood ratios, $[^{68}\text{Ga}]\text{Ga-YW-11}$ exhibited the lowest ratio at all time points (0.02–0.04) when compared to $[^{68}\text{Ga}]\text{Ga-YW-15}$ and $[^{68}\text{Ga}]\text{Ga-YW-18}$. Brain-to-blood ratios of $[^{68}\text{Ga}]\text{Ga-YW-15}$ and $[^{68}\text{Ga}]\text{Ga-YW-18}$ were comparable at 2 min (0.04 and 0.03, respectively), 1 h (0.07 and 0.08, respectively), and at 2 h (0.14 and 0.10, respectively). Table S1 shows the full biodistribution profiles of ^{68}Ga -labeled radiotracers in CD-1 mice. High uptake was observed in the lung and liver for $[^{68}\text{Ga}]\text{Ga-YW-11}$, in which the radioactive uptake effectively cleared out from the lung and remained persistent in the liver at 2 h. $[^{68}\text{Ga}]\text{Ga-YW-15}$ also had high lung and liver uptake initially, and lung uptake rapidly cleared out, while liver

uptake remained high at 2 h. [^{68}Ga]Ga-YW-18 had the best non-target tissue clearance with the lung and liver uptake of less than 2% ID/g at 2 h.

DISCUSSION

The present studies report a series of TACN-based BFCs radiolabeled with ^{68}Ga as the potential PET imaging agent for amyloid β . The selective staining of the novel BFCs toward amyloid aggregates was investigated in *in vitro* studies using 5xFAD mice. Intense fluorescence signals and good Pearson's correlation coefficients with Congo Red or HJ3.4 antibody staining suggest that YW-13, YW-15, and YW-18 can bind to the amyloid β in the brain sections specifically. In our recent reports, we have shown that the free BFCs and the corresponding Cu(II) complexes show similar binding affinities and specificity for the amyloid plaques, as confirmed by both fluorescence microscopy and autoradiography.^{30,32–36} In addition, other studies have reported that different A β -binding chelators and their corresponding Ga(III) complexes exhibit similar binding affinities (within 3–8 fold) for A β aggregates.^{17,24} While ideally *in vitro* studies should be performed to clearly evaluate the effect of Ga chelation on the amyloid-binding affinity of newly developed chelators, we considered the previous results support our hypothesis that the designed BFCs and their Ga(III) complexes should exhibit similar amyloid-binding affinities, at least for the initial autoradiography and biodistribution studies described herein.

Radiolabeling with ^{68}Ga was efficient, and a high radiochemical yield of 95% was achieved within 15 min of heating at 95 °C. Harsh conditions are standard for ^{68}Ga labeling as often required to achieve rapid radiolabeling due to the short half-life of 68 min. However, heating at elevated temperature can have detrimental effects on larger biomolecules such as proteins, which is not the case for our studies. All ^{68}Ga conjugates were subsequently used without further purification. The retention times in radio-HPLC correspond to the molecular weight of each product with YW-13 at 9:01 min, YW-15 at 10:40 min, and YW-18 at 11:01 min upon the addition of an extra amyloid-binding motif. YW-11 has two retention times—12:47 min that corresponds to the original trivalent radiolabeled complex and 10:41 min for the bivalent product after degradation. Ligand lipophilicity was assessed to predict non-specific binding due to increased hydrophobicity. In our studies, [^{68}Ga]Ga-YW-13 has the lowest $\log D_{\text{oct}}$ with only one amyloid-binding motif in the backbone. The addition of bulky substituents in the backbone resulted in increased hydrophobicity of the compound; thus, increased $\log D_{\text{oct}}$ for bivalent and trivalent radiolabeled complexes were observed. This was confirmed in our studies that [^{68}Ga]Ga-YW-11 has a higher $\log D_{\text{oct}}$ compared to [^{68}Ga]Ga-YW-15 likely due to the additional amyloid-binding motifs. On the other hand, [^{68}Ga]Ga-YW-18 has a higher $\log D_{\text{oct}}$ compared to [^{68}Ga]Ga-YW-15 due to its complexation with ^{68}Ga to form a neutral species.

Autoradiographic images confirmed the specific binding of ^{68}Ga -radiolabeled complexes toward amyloid β . The intensity ratios of 5xFAD to WT brain section signals indicated that the introduction of extra amyloid β targeting moieties increased the affinity of BFCs to amyloid plaques, although the overall size and charge of the ^{68}Ga -radiolabeled complexes can affect the amyloid-binding affinity. This corresponds to the previous studies that indicate the ability of multivalent ligands to enhance binding affinity.^{16,34} For example, a comparison study

of $^{99\text{m}}\text{Tc}$ -hydroxamamide ($^{99\text{m}}\text{Tc}$ -Ham) complexes with monovalent and bivalent amyloid ligand was performed, and autoradiography of Tg2576 APP transgenic mice showed a higher binding affinity for amyloid β of the bivalent complex.¹⁶ Another study by Cho et al. also confirmed the multivalent ligand effect on A β binding as presented in about 1.5-fold increase in average intensities of the 5xFAD brain sections after the treatment of mono- or divalent ^{64}Cu complexes.³⁴

Biodistribution studies in normal CD-1 mice revealed low brain uptake of novel ^{68}Ga -radiolabeled complexes *in vivo*. The low brain uptake of novel ^{68}Ga -radiolabeled BFCs supports that they are suitable for the imaging of amyloid β on the walls of cerebral blood vessels, not those in the parenchymal brain tissues. Zha et al. have evaluated styrylpyridine derivatives radiolabeled with ^{68}Ga for the imaging of amyloids in CAA that displayed specific binding toward A β plaques and had low brain uptake (0.1–0.3% ID/g at 2 min).¹⁷ Their reported brain uptake values were comparable to the brain uptake of [^{68}Ga]Ga-YW-11 (0.10 \pm 0.03% ID/g at 2 min), [^{68}Ga]Ga-YW-15 (0.26 \pm 0.12% ID/g at 2 min), and [^{68}Ga]Ga-YW-18 (0.33 \pm 0.12% ID/g at 2 min), thus highlighting the potential of novel radiotracers to selectively label amyloid β on the vessel walls.

CONCLUSIONS

In conclusion, novel TACN complexes with multivalent amyloid-binding groups present useful molecular imaging probes for CAA due to their high binding affinity for A β plaques. Histological staining of 5xFAD mouse brain sections illustrated the specific binding of ^{68}Ga bivalent complexes to amyloid β . *In vitro* autoradiography indicated the enhancement of the binding affinity by multivalency as reflected by the increased intensity ratios of 5xFAD brain sections compared to WT age-matched ones. The compounds exhibited low brain uptake *in vivo* which can be useful for the development of CAA-specific imaging agents to differentiate CAA from AD. Taken together, these findings strongly suggest that ^{68}Ga bivalent complexes are good imaging probes targeting amyloid aggregates deposited in CAA and peripheral amyloidosis.

EXPERIMENTAL SECTION

General Methods. All solvents and reagents used in this study were obtained from Sigma Aldrich (St. Louis, MO) or Fisher Scientific (Pittsburgh, PA). Buffers used for radiolabeling were prepared in chelexed Milli-Q water which was filtered through a 0.22 μm nylon filter. A Varian Mercury-300 spectrometer or a VARIAN UNITY Inova 400 spectrometer was utilized to record ^1H (300 MHz) NMR spectra. A VARIAN VXR 500 with a UNITY INOVA Console spectrometer was used to record ^{13}C (126 MHz) NMR spectra. Chemical shifts are reported in parts per million and referenced to residual solvent resonance peaks. Radio-TLC detection was accomplished using a Bioscan 200 imaging scanner (Bioscan, Inc., Washington, DC). Radioactive samples were counted on a Beckman Gamma 8000 counter containing a NaI crystal (Beckman Instruments, Inc., Irvine, CA). A two-solvent reversed-phase HPLC system was used to evaluate the radiolabeling efficiency with water [0.05% trifluoroacetic acid (TFA)] and acetonitrile (0.05% TFA). HPLC used a Kinetex (Phenomenex) C-18 column (5 μm , 4.6 \times 150 mm I.D.). The HPLC instrument was composed of UV absorbance detectors set at 220 and 280 nm, a NaI radiotracer detector, and a

photodiode array detector. A gradient elution with acetonitrile (0.1% TFA) 0–100% buffer mobile phase over the course of 13 min and a 1 mL/min flow rate was developed for radiochemical purity profiling.

Syntheses of BFCs. *YW-11.* Paraformaldehyde (0.043 g, 1.4 mmol) was added to a solution of TACN (0.0875 g, 0.68 mmol) in 1,4-dioxane (15 mL), followed by heating under reflux for 1 h. 2-(4-Hydroxy-3-methoxy)-benzothiazole (0.36 g, 1.4 mmol) in 1,4-dioxane (10 mL) was then added, the solution was refluxed for an additional 72 h, and then cooled to room temperature. After the removal of the solvent, an orange-yellow residue was collected and purified by flash column chromatography using DCM/MeOH (30:1). The resulting yellow solution was dried and a yellow precipitate formed (71 mg, yield 11%). ¹H NMR (300 MHz, CDCl₃) δ 8.0 (d, *J* = 8.1 Hz, 3H), 7.8 (d, *J* = 7.9 Hz, 3H), 7.6 (s, 3H), 7.4 (t, *J* = 7.7 Hz, 3H), 7.3 (dd, *J* = 14.2, 6.2 Hz, 6H), 4.0 (s, 9H), 3.9 (s, 6H), 3.0 (s, 12H). ¹³C NMR (126 MHz, CDCl₃) δ 168.2, 154.0, 148.0, 134.8, 126.7, 125.4, 125.3, 122.9, 121.9, 110.3, 56.4, 30.0. ESI-MS: calcd for [M + H]⁺, 937.2831; found, 937.2883.

YW-13. The synthesis of **YW-13** was conducted as previously described.³⁵

YW-15. Paraformaldehyde (0.067 g, 2.2 mmol) was added to a solution of TACN (0.106 g, 0.82 mmol) in EtOH (10 mL), followed by heating under reflux for 1 h. 2-(4-Hydroxy-3-methoxy)-benzothiazole (0.32 g, 1.23 mmol) in EtOH (10 mL) was then added, followed by an additional 36 h of reflux, and then the resulting mixture was cooled to room temperature. After the removal of the solvent, an orange-yellow residue was collected. This residue was purified to give a yellow solution by Combi-Flash (reverse-phase) using MeCN/H₂O/TFA (45:55:0.1), followed by the neutralization process with NaHCO₃, and extraction with dichloromethane. The resulting solution was then dried and a yellow solid formed (21 mg, yield 4%). ¹H NMR (499 MHz, CDCl₃) δ 8.0 (d, *J* = 8.1 Hz, 2H), 7.8 (d, *J* = 7.9 Hz, 2H), 7.6 (s, 2H), 7.4 (t, *J* = 7.7 Hz, 2H), 7.4 (s, 2H), 7.3 (t, *J* = 7.6 Hz, 2H), 4.0 (s, 6H), 3.8 (s, 4H), 3.1–2.7 (m, 11H). ¹³C NMR (126 MHz, CDCl₃) δ 154.4, 148.5, 135.0, 126.4, 124.9, 124.3, 124.1, 122.9, 122.2, 121.7, 109.9, 56.4, 53.7. HR-ESI-MS: calcd for [M + H]⁺, 668.2321; found, 668.2370.

YW-16. *tert*-Butyl bromoacetate (33.5 mg, 0.17 mmol) in 5 mL of MeCN was added to a suspension of **YW-15** (95.6 mg, 0.14 mmol) and sodium carbonate (18 mg, 0.17 mmol) in 15 mL of 1:1 (v:v) MeCN/DCM, followed by stirring of the reaction mixture for 20 h at room temperature. After the removal of the solvent, an orange-yellow residue was collected. This residue was purified to give a yellow solution by Combi-Flash (reverse-phase) using MeCN/H₂O/TFA (60:40:0.1), followed by the neutralization process with NaHCO₃, and extraction with dichloromethane. The resulting solution was then dried and a yellow solid formed (76 mg, yield 68%). ¹H NMR (300 MHz, CDCl₃) δ 8.0 (d, *J* = 8.1 Hz, 2H), 7.9 (d, *J* = 7.8 Hz, 2H), 7.7 (s, 2H), 7.5–7.4 (m, 4H), 7.4 (t, *J* = 7.6 Hz, 2H), 4.2 (d, *J* = 23.9 Hz, 4H), 3.8 (s, 6H), 3.2 (d, *J* = 82.9 Hz, 15H), 1.3 (s, 9H). ¹³C NMR (126 MHz, CDCl₃) δ 171.0, 154.1, 148.5, 134.9, 126.5, 124.9, 122.8, 121.8, 110.2, 81.4, 56.4, 28.4, 28.0. HR-ESI-MS: calcd for [M + H]⁺, 782.3001; found, 782.3041.

YW-18. A reaction mixture of **YW-16** (76 mg, 0.10 mmol) and 5 mL of 6 M hydrochloric acid was stirred and refluxed for 18 h. After the removal of the solvent, a yellow residue was collected. This residue was purified to give a yellow solution by

Combi-Flash (reverse-phase) using MeCN/H₂O/TFA (50:50:0.1), followed by the neutralization process with NaHCO₃, and extraction with dichloromethane. The resulting solution was then dried and a yellow solid formed (19.4 mg, yield 28%). ¹H NMR (499 MHz, CD₃OD) δ 7.9 (d, *J* = 8.1 Hz, 2H), 7.8 (d, *J* = 7.9 Hz, 2H), 7.6 (s, 2H), 7.5 (s, 2H), 7.4 (t, *J* = 7.6 Hz, 2H), 7.3 (t, *J* = 7.5 Hz, 2H), 4.1 (s, 4H), 3.8 (d, *J* = 3.6 Hz, 7H), 3.4 (d, *J* = 2.5 Hz, 2H), 3.3 (d, *J* = 2.0 Hz, 15H). ¹³C NMR (126 MHz, CD₃OD) δ 168.6, 153.5, 148.4, 134.5, 126.6, 125.3, 122.8, 122.1, 121.7, 110.3, 55.6, 54.0, 50.7. HR-ESI-MS: calcd for [M + H]⁺, 726.2375; found, 726.2422.

Histological Staining of 5xFAD Mouse Brain Sections. 5xFAD mouse brain sections (11-month-old) were used to evaluate the binding affinity for amyloid aggregates. The sections were blocked for 10 min with bovine serum albumin (2% BSA in PBS, pH 7.4), followed by 30 min incubation with BFCs dissolved in PBS. The sections were subsequently stained for 30 min in a 2 μM Congo Red solution. Brain sections were incubated for 4 min with BSA, rinsed three times with PBS (each cycle 2 min) followed by 2 min DI water wash, and then mounted with non-fluorescent mounting media in order to remove non-specific binding. To further confirm the specificity of novel BFCs toward amyloid β, the AF594-conjugated anti-Aβ antibody (AF594-HJ3.4 antibody) solution (1 μg/mL) was added to mouse brain sections (11-month-old) for 1 h at room temperature, followed by the same incubation and wash steps as previously described for Congo Red staining. The antibodies were labeled with dye Cy594 via the Mix-n-Stain CF 594 Antibody Labeling Kit (Sigma Aldrich). A Zeiss LSM 7010 confocal fluorescent microscope and an Invitrogen EVOS FL Auto 2 Imaging System (Thermo Fisher, USA) were used to image stained brain sections. Colocalization analysis and determination of the Pearson's correlation coefficient were performed using ImageJ (1.52, public domain) software.

Radionuclide Production. ⁶⁸Ga was produced using a commercial ⁶⁸Ge/⁶⁸Ga generator (Eckert & Ziegler, Berlin, Germany) system as described.³⁷ Briefly, the elution of ⁶⁸Ga from the generator was carried out in 5 mL of 0.1 M HCl. The eluted activity was added to a Strata XC strong cation exchange column 30 mg/mL 33 μm (Phenomenex, Torrance, CA) which effectively retains the activity. 0.8 mL of 98% acetone (0.02 M HCl) was added to the column, and the eluent was collected in a 1.5 mL Eppendorf tube, followed by heating at 95 °C for 15 min until 10–20 μL ⁶⁸Ga was achieved.

Radiolabeling of BFCs. Efficient labeling with ⁶⁸Ga was accomplished by adding 20 μL of 1 mM ligand in DMSO to 7.4 MBq (200 μCi) of ⁶⁸Ga in 50 μL of 0.1 M NH₄OAc (pH 5.5) at 95 °C for 15 min. Radiolabeled products were evaluated using HPLC. A gradient from 0 to 100% and acetonitrile (0.1% TFA) was used with a flow rate of 1 mL/min in 13 min.

Lipophilicity Studies. An equal volume of *n*-octanol and PBS 1X was added to 10 Eppendorf tubes (500 μL each). An aliquot of 5–10 μL radiolabeled ⁶⁸Ga complexes was added to each tube, vortexed, and incubated for 1 h at room temperature with moderate shaking. The mixtures were then allowed to sit still in the bunker for 30 min for the two layers—aqueous and *n*-octanol to separate. 100 μL from each layer was collected in tubes, and the radioactivity was counted using an automated gamma counter. The counts (in cpm) were corrected for radioactive decay. logD_{oct} was calculated to be the logarithm of the ratio of (radioactivity of the organic phase)/(radioactivity of the aqueous phase). The average of 10

replicate values was recorded as the $\log D_{\text{oct}}$ for each compound.

In Vitro Autoradiography Studies. Brain sections of 5xFAD transgenic mice and WT mice (11-month-old) were immersed in a cryo-protectant solution. Brain sections were rinsed three times with 100% PBS, and each section was placed in each well of the 12-well plate. 3.7 MBq (100 μCi) ^{68}Ga -labeled compounds in 1 mL of PBS were added to the wells, and the well plates were incubated at room temperature for 1 h. Specific binding of ^{68}Ga -labeled BFCs toward amyloid plaques was evaluated in blocking studies by co-incubating with excess 2-(4-hydroxyphenyl)-benzothiazole. Brain sections were then rinsed 3×2 min in ice-cold PBS before being removed. Sections were placed on glass microscope slides and completely air-dried at room temperature. The slides were placed in an imaging cassette in contact with a phosphor-imaging screen plate (GE Healthcare Life Sciences). The screen was exposed overnight at $-20\text{ }^\circ\text{C}$ and then scanned on a phosphor-imager plate scanner (Storm 840). ImageJ (1.53, public domain) software was used to review the images.

Biodistribution Studies. All animals involved were obtained from Charles River Laboratories (Wilmington, MA). For animal research, the Guidelines for Care and Use of Research Animals established by the Animal Studies Committee of Washington University School of Medicine and the Division of Comparative Medicine were strictly followed. CD-1 female mice (5–7 weeks of age) were intravenously injected with 10 μCi (0.37 MBq) of ^{68}Ga -radiotracers in 100 μL of saline. Mice were sacrificed after a period of 2, 60, and 240 min after intravenous injection. Organs of interest (blood, lung, liver, kidney, muscle, brain, bone, and tail) were harvested and counted on a gamma counter. Radioactivity concentrations were decay-corrected and expressed as percent injected dose per gram (%ID/g).

Statistical Analysis. All values are expressed as mean \pm SD. Quantitative data were analyzed using Prism software version 9 (GraphPad Software, La Jolla, CA). One-way analysis of variance and Student's *t*-test are statistical methods used in the study, in which a *p*-value of 0.05 or lower is considered statistically significant.

■ ASSOCIATED CONTENT

SI Supporting Information

The Supporting Information is available free of charge at <https://pubs.acs.org/doi/10.1021/acsomega.2c02369>.

Characterization of novel BFCs using ^1H NMR, ^{13}C NMR, and HR ESI-MS; HPLC chromatograms showing the ^{68}Ga -labeled radiotracer; and biodistribution profile of ^{68}Ga -labeled radiotracers in CD-1 mice (PDF)

■ AUTHOR INFORMATION

Corresponding Authors

Liviu M. Mirica – Department of Chemistry, University of Illinois at Urbana-Champaign, Urbana, Illinois 61801, United States; Hope Center for Neurological Disorders, Washington University School of Medicine, St. Louis, Missouri 63110, United States; orcid.org/0000-0003-0584-9508; Email: mirica@illinois.edu

Buck E. Rogers – Department of Radiation Oncology, Washington University School of Medicine, St. Louis, Missouri 63108, United States; orcid.org/0000-0001-8189-1797; Email: b.rogers@wustl.edu

Authors

Truc T. Huynh – Department of Radiation Oncology, Washington University School of Medicine, St. Louis, Missouri 63108, United States; Department of Chemistry, Washington University, St. Louis, Missouri 63130, United States

Yujue Wang – Department of Chemistry, University of Illinois at Urbana-Champaign, Urbana, Illinois 61801, United States

Karna Terpstra – Department of Chemistry, University of Illinois at Urbana-Champaign, Urbana, Illinois 61801, United States

Hong-Jun Cho – Department of Chemistry, University of Illinois at Urbana-Champaign, Urbana, Illinois 61801, United States

Complete contact information is available at:

<https://pubs.acs.org/10.1021/acsomega.2c02369>

Notes

The authors declare no competing financial interest.

■ ACKNOWLEDGMENTS

This work was supported by the NIH (R01GM114588 to L.M.M.). We thank Nikki Fettig and Lori Strong from the Washington University Small Animal imaging facility for providing technical assistance for animal studies.

■ REFERENCES

- (1) Vinters, H. V. Cerebral amyloid angiopathy. A critical review. *Stroke* **1987**, *18*, 311–324.
- (2) Viswanathan, A.; Greenberg, S. M. Cerebral amyloid angiopathy in the elderly. *Ann. Neurol.* **2011**, *70*, 871–880.
- (3) Murphy, M. P.; LeVine, H., 3rd Alzheimer's disease and the amyloid-beta peptide. *J. Alzheimer's Dis.* **2010**, *19*, 311–323.
- (4) Ellis, R. J.; Olichney, J. M.; Thal, L. J.; Mirra, S. S.; Morris, J. C.; Beekly, D.; Heyman, A. Cerebral amyloid angiopathy in the brains of patients with Alzheimer's disease: the CERAD experience, Part XV. *Neurology* **1996**, *46*, 1592–1596.
- (5) Jellinger, K. A. Alzheimer disease and cerebrovascular pathology: an update. *J. Neural Transm.* **2002**, *109*, 813–836.
- (6) Brenowitz, W. D.; Nelson, P. T.; Besser, L. M.; Heller, K. B.; Kukull, W. A. Cerebral amyloid angiopathy and its co-occurrence with Alzheimer's disease and other cerebrovascular neuropathologic changes. *Neurobiol. Aging* **2015**, *36*, 2702–2708.
- (7) Voropai, E. S.; Samtsov, M. P.; Kaplevskii, K. N.; Maskevich, A. A.; Stepuro, V. I.; Povarova, O. I.; Kuznetsova, I. M.; Turoverov, K. K.; Fink, A. L.; Uverskii, V. N. Spectral Properties of Thioflavin T and Its Complexes with Amyloid Fibrils. *J. Appl. Spectrosc.* **2003**, *70*, 868–874.
- (8) Ono, M.; Haratake, M.; Mori, H.; Nakayama, M. Novel chalcones as probes for in vivo imaging of beta-amyloid plaques in Alzheimer's brains. *Bioorg. Med. Chem.* **2007**, *15*, 6802–6809.
- (9) Yang, F.; Lim, G. P.; Begum, A. N.; Ubeda, O. J.; Simmons, M. R.; Ambegaokar, S. S.; Chen, P. P.; Kaye, R.; Glabe, C. G.; Frautschy, S. A.; Cole, G. M. Curcumin inhibits formation of amyloid beta oligomers and fibrils, binds plaques, and reduces amyloid in vivo. *J. Biol. Chem.* **2005**, *280*, 5892–5901.
- (10) Eckroat, T. J.; Mayhoub, A. S.; Garneau-Tsodikova, S. Amyloid- β probes: Review of structure-activity and brain-kinetics relationships. *Beilstein J. Org. Chem.* **2013**, *9*, 1012–1044.
- (11) Klunk, W. E.; Engler, H.; Nordberg, A.; Wang, Y.; Blomqvist, G.; Holt, D. P.; Bergström, M.; Savitcheva, I.; Huang, G.-F.; Estrada, S.; Ausén, B.; Debnath, M. L.; Barletta, J.; Price, J. C.; Sandell, J.; Lopresti, B. J.; Wall, A.; Koivisto, P.; Antoni, G.; Mathis, C. A.; Långström, B. Imaging brain amyloid in Alzheimer's disease with Pittsburgh Compound-B. *Ann. Neurol.* **2004**, *55*, 306–319.

- (12) Martins, A. F.; Morfin, J. F.; Kubičková, A.; Kubiček, V.; Buron, F.; Suzenet, F.; Salerno, M.; Lazar, A. N.; Duyckaerts, C.; Arlicot, N.; Guilloteau, D.; Geraldos, C. F.; Tóth, E. PiB-Conjugated, Metal-Based Imaging Probes: Multimodal Approaches for the Visualization of β -Amyloid Plaques. *ACS Med. Chem. Lett.* **2013**, *4*, 436–440.
- (13) Johnson, K. A.; Sperling, R. A.; Gidicsin, C. M.; Carmasin, J. S.; Maye, J. E.; Coleman, R. E.; Reiman, E. M.; Sabbagh, M. N.; Sadowsky, C. H.; Fleisher, A. S.; Murali Doraiswamy, P.; Carpenter, A. P.; Clark, C. M.; Joshi, A. D.; Lu, M.; Grundman, M.; Mintun, M. A.; Pontecorvo, M. J.; Skovronsky, D. M. AV45-A11 study group, Florbetapir (F18-AV-45) PET to assess amyloid burden in Alzheimer's disease dementia, mild cognitive impairment, and normal aging. *Alzheimer's Dement.* **2013**, *9*, S72–S83.
- (14) Sabri, O.; Seibyl, J.; Rowe, C.; Barthel, H. Beta-amyloid imaging with florbetaben. *Clin. Transl. Imaging* **2015**, *3*, 13–26.
- (15) Heurling, K.; Leuzy, A.; Zimmer, E. R.; Lubberink, M.; Nordberg, A. Imaging β -amyloid using [18F]flutemetamol positron emission tomography: from dosimetry to clinical diagnosis. *Eur. J. Nucl. Med. Mol. Imaging* **2016**, *43*, 362–373.
- (16) Iikuni, S.; Ono, M.; Watanabe, H.; Matsumura, K.; Yoshimura, M.; Harada, N.; Kimura, H.; Nakayama, M.; Saji, H. Enhancement of Binding Affinity for Amyloid Aggregates by Multivalent Interactions of 99mTc-Hydroxamate Complexes. *Mol. Pharmaceutics* **2014**, *11*, 1132–1139.
- (17) Zha, Z.; Song, J.; Choi, S. R.; Wu, Z.; Ploessl, K.; Smith, M.; Kung, H. 68Ga-Bivalent Polypegylated Styrylpyridine Conjugates for Imaging $A\beta$ Plaques in Cerebral Amyloid Angiopathy. *Bioconjugate Chem.* **2016**, *27*, 1314–1323.
- (18) Fani, M.; André, J. P.; Maecke, H. R. 68Ga-PET: a powerful generator-based alternative to cyclotron-based PET radiopharmaceuticals. *Contrast Media Mol. Imaging* **2008**, *3*, 53–63.
- (19) Prata, M. I. Gallium-68: A new trend in PET radiopharmacy. *Curr. Radiopharm.* **2012**, *5*, 142–149.
- (20) Watanabe, H.; Ono, M.; Iikuni, S.; Yoshimura, M.; Matsumura, K.; Kimura, H.; Saji, H. A 68Ga complex based on benzofuran scaffold for the detection of β -amyloid plaques. *Bioorg. Med. Chem. Lett.* **2014**, *24*, 4834–4837.
- (21) Cressier, D.; Dhilly, M.; Cao Pham, T. T.; Fillesoy, F.; Gourand, F.; Maïza, A.; Martins, A. F.; Morfin, J.-F.; Geraldos, C. F. G. C.; Tóth, É.; Barré, L. Gallium-68 Complexes Conjugated to Pittsburgh Compound B: Radiolabeling and Biological Evaluation. *Mol. Imaging Biol.* **2016**, *18*, 334–343.
- (22) Asti, M.; Ferrari, E.; Croci, S.; Atti, G.; Rubagotti, S.; Iori, M.; Capponi, P. C.; Zerbini, A.; Saladini, M.; Versari, A. Synthesis and Characterization of 68Ga-Labeled Curcumin and Curcuminoid Complexes as Potential Radiotracers for Imaging of Cancer and Alzheimer's Disease. *Inorg. Chem.* **2014**, *53*, 4922–4933.
- (23) Rubagotti, S.; Croci, S.; Ferrari, E.; Iori, M.; Capponi, P. C.; Lorenzini, L.; Calzà, L.; Versari, A.; Asti, M. Affinity of (nat/68)Ga-Labeled Curcumin and Curcuminoid Complexes for β -Amyloid Plaques: Towards the Development of New Metal-Curcumin Based Radiotracers. *Int. J. Mol. Sci.* **2016**, *17*, 1480.
- (24) Chauhan, K.; Datta, A.; Adhikari, A.; Chuttani, K.; Kumar Singh, A.; Mishra, A. K. (68)Ga based probe for Alzheimer's disease: synthesis and preclinical evaluation of homodimeric chalcone in β -amyloid imaging. *Org. Biomol. Chem.* **2014**, *12*, 7328–7337.
- (25) Lange, J. L.; Hayne, D. J.; Roselt, P.; McLean, C. A.; White, J. M.; Donnelly, P. S. A gallium(III) Schiff base-curcumin complex that binds to amyloid- β plaques. *J. Inorg. Biochem.* **2016**, *162*, 274–279.
- (26) Zhang, Q.; Zhao, X.; Lei, P.; Kung, H. F.; Yang, Z.; Zhu, L.; Wang, S.; Zhu, H.; Meng, X.; Duan, Y.; Sun, L.; Pan, J.; Ma, R.; Hong, H.; Zhao, X.; Demchuk, A.; Smith, E. E.; Wang, Y. Evaluating [68Ga]Ga-p14-032 as a Novel PET Tracer for Diagnosis Cerebral Amyloid Angiopathy. *Front. Neurol.* **2021**, *12*, No. 702185.
- (27) Tsionou, M. I.; Knapp, C. E.; Foley, C. A.; Munteanu, C. R.; Cakebread, A.; Imberti, C.; Eykyn, T. R.; Young, J. D.; Paterson, B. M.; Blower, P. J.; Ma, M. T. Comparison of macrocyclic and acyclic chelators for gallium-68 radiolabelling. *RSC Adv.* **2017**, *7*, 49586–49599.
- (28) Ray Banerjee, S.; Chen, Z.; Pullambhatla, M.; Lisok, A.; Chen, J.; Mease, R. C.; Pomper, M. G. Preclinical Comparative Study of (68)Ga-Labeled DOTA, NOTA, and HBED-CC Chelated Radiotracers for Targeting PSMA. *Bioconjugate Chem.* **2016**, *27*, 1447–1455.
- (29) Xia, Y.; Zeng, C.; Zhao, Y.; Zhang, X.; Li, Z.; Chen, Y. Comparative evaluation of (68)Ga-labelled TATEs: the impact of chelators on imaging. *EJNMMI Res.* **2020**, *10*, 36.
- (30) Bandara, N.; Sharma, A. K.; Krieger, S.; Schultz, J. W.; Han, B. H.; Rogers, B. E.; Mirica, L. M. Evaluation of 64Cu-Based Radiopharmaceuticals that Target $A\beta$ Peptide Aggregates as Diagnostic Tools for Alzheimer's Disease. *J. Am. Chem. Soc.* **2017**, *139*, 12550–12558.
- (31) Sharma, A. K.; Schultz, J. W.; Prior, J. T.; Rath, N. P.; Mirica, L. M. Coordination Chemistry of Bifunctional Chemical Agents Designed for Applications in 64Cu PET Imaging for Alzheimer's Disease. *Inorg. Chem.* **2017**, *56*, 13801–13814.
- (32) Huang, Y.; Cho, H.-J.; Bandara, N.; Sun, L.; Tran, D.; Rogers, B. E.; Mirica, L. M. Metal-chelating benzothiazole multifunctional compounds for the modulation and 64Cu PET imaging of $A\beta$ aggregation. *Chem. Sci.* **2020**, *11*, 7789–7799.
- (33) Sun, L.; Cho, H.-J.; Sen, S.; Arango, A. S.; Huynh, T. T.; Huang, Y.; Bandara, N.; Rogers, B. E.; Tajkhorshid, E.; Mirica, L. M. Amphiphilic Distyrylbenzene Derivatives as Potential Therapeutic and Imaging Agents for Soluble and Insoluble Amyloid β Aggregates in Alzheimer's Disease. *J. Am. Chem. Soc.* **2021**, *143*, 10462–10476.
- (34) Cho, H.-J.; Huynh, T. T.; Rogers, B. E.; Mirica, L. M. Design of a multivalent bifunctional chelator for diagnostic 64Cu PET imaging in Alzheimer's disease. *Proc. Natl. Acad. Sci. U. S. A.* **2020**, *117*, 30928–30933.
- (35) Wang, Y.; Huynh, T. T.; Bandara, N.; Cho, H.-J.; Rogers, B. E.; Mirica, L. M. 2-(4-Hydroxyphenyl)benzothiazole dicarboxylate ester TACN chelators for 64Cu PET imaging in Alzheimer's disease. *Dalton Trans.* **2022**, *51*, 1216–1224.
- (36) Wang, Y.; Huynh, T. T.; Cho, H.-J.; Wang, Y.-C.; Rogers, B. E.; Mirica, L. M. Amyloid β -Binding Bifunctional Chelators with Favorable Lipophilicity for 64Cu Positron Emission Tomography Imaging in Alzheimer's Disease. *Inorg. Chem.* **2021**, *60*, 12610–12620.
- (37) Ocak, M.; Antretter, M.; Knopp, R.; Kunkel, F.; Petrik, M.; Bergisadi, N.; Decristoforo, C. Full automation of 68Ga labelling of DOTA-peptides including cation exchange prepurification. *Appl. Radiat. Isot.* **2010**, *68*, 297–302.